

Observation of Macroscopic Spin Phenomena in Nanometer-Scale Magnets

D. D. Awschalom, M. A. McCord, and G. Grinstein

IBM Watson Research Center, P.O. Box 218, Yorktown Heights, New York 10598

(Received 17 May 1990)

A scanning tunneling microscope is used to locally deposit arrays of nanometer-scale magnets directly within the superconducting planar input coil of an integrated dc SQUID microsusceptometer. Low-temperature frequency-dependent magnetic-susceptibility measurements reveal a narrow resonance which grows and becomes independent of decreasing temperature. Studies as a function of magnet volume, spacing, and applied field are compared to recent predictions for magnetic macroscopic quantum tunneling in small particles.

PACS numbers: 73.40.Gk, 05.40.+j, 75.50.Bb, 75.60.Jp

The last decade's theoretical and experimental progress in the understanding of macroscopic quantum tunneling (MQT) and the role of dissipation in Josephson devices represents a milestone in the elucidation of quantum phenomena.^{1,2} Recently, small ferromagnetic particles were proposed as another system where quantum mechanics is likely to produce measurable manifestations on the macroscopic level.³ Unlike bulk magnets where the formation and movement of magnetic domains is central to the dynamics, a ferromagnet of size significantly less than the width of a domain wall at low temperatures has all of its spins rigidly aligned, forming a single coherent "superparamagnetic" particle. Within this regime it is predicted that the magnetization \mathbf{M} , which even for nanometer-scale particles contains 10^5 – 10^6 spins, can tunnel between local energy minima separated by a barrier determined by the magnetic anisotropy.^{3,4} This raises the intriguing prospect of using magnetic-susceptibility measurements to observe directly the coherent oscillations associated with macroscopic quantum tunneling of the magnetization.

In this paper we report measurements of the low-temperature spin dynamics of nanometer-scale magnets configured in regular arrays. The central observation is that as the temperature T is lowered, a well-defined peak at a frequency $\omega_c \sim 500$ Hz appears in the frequency-dependent magnetic susceptibility $\chi(\omega)$ at $T \sim 200$ mK and becomes independent of temperature for $T < T_c \sim 75$ mK. The resonance does not appear in arrays whose interparticle spacing is sufficiently small, implying that it is associated with the dynamics of the individual particles and can be suppressed by strong interparticle interactions. This behavior qualitatively suggests the occurrence of magnetic quantum tunneling in the nanometer-scale magnets. Several additional experimental tests, notably the dependence of ω_c on particle volume and the effect of a magnetic field, were performed to test this hypothesis. We find it difficult to reconcile the results with the current theoretical picture of magnetic MQT.

The experiment utilizes a combination of two distinct

superconducting integrated circuits which are interconnected to form a miniature susceptometer.⁵ In order to reduce the effects of stray magnetic fields, the microfabricated pickup loop structure consists of a pair of superconducting square counterwound Pb loops, 25 μm on a side, one of which contains the magnetic nanometer-scale structures. In addition, a center-tapped Nb field coil which takes a single square turn around each pickup loop is used to apply a small ac magnetic field (~ 30 mG) for susceptibility measurements, as well as static dc magnetic fields. This gradiometer assembly is connected with short superconducting Al wire bonds to the five-turn spiral input transformer of an integrated planar dc SQUID operating in a conventional flux-locked feedback mode with room-temperature electronics. Both circuits are mounted on a sapphire carrier which rests upon a copper block attached directly to the mixing chamber of a dilution refrigerator and cooled to $T \sim 20$ mK with Mumetal shields. The experiment and necessary superconducting electronics are enclosed within a rf-tight box of copper-laminated fiberglass plated with lead-tin solder for addition shielding, yielding a magnetic-flux noise $< 10^{-6} \phi_0 / \sqrt{\text{Hz}}$.

Nanometer-scale magnets were fabricated using a modified scanning tunneling microscope (STM) to locally decompose iron pentacarbonyl molecules $[\text{Fe}(\text{CO})]$ directly into a single gradiometer pickup loop.⁶ After the deposition of an 80-nm gold film over the active area of both susceptometer coils, the STM tip was coarsely positioned using an optical microscope and then centered by directly imaging the coil. A computer regulates the magnet growth by maintaining a constant height between the STM tip and the growing structure, and terminates at a desired height (25–100 nm) by fully retracting the tip. The structure diameter (10–30 nm) is determined by the voltage applied between the tip and the sample. These sample dimensions are small compared to the domain-wall thicknesses for crystalline ferromagnets.⁷ Scanning electron microscopy (SEM) shows the arrays to contain ellipsoidal particles having a very narrow size distribution, but accurate determina-

tions of the smallest dimensions are limited to $\sim 10\%$ by the resolution of the SEM and carbon contamination buildup during inspection. Arrays containing 50 to 150 magnets with spacings from 0.10 to 1.3 μm are grown at ambient temperature under a pressure of 160 mTorr Fe(CO), requiring approximately 100 ms/structure. Although the atomic composition cannot be precisely determined, microprobe analysis of these structures and Auger analysis of similar depositions indicate that the magnets contain $\sim 60\%$ iron with the remainder being primarily carbon.

Figure 1 shows $|\chi(\omega)|$ as a function of ω at $T=22.5$ mK for arrays of magnetic particles of three different sizes and 1- μm spacing. Each of the data sets shows a well-defined resonant peak at a frequency ω_c which moves to lower frequencies with increasing particle volume. The amplitudes of the magnetic signals are roughly consistent with the expected number of iron spins ($\sim 10^7$) in the array. The resonances sit upon a background which increases with decreasing frequency, typical of activated spin-relaxation processes which occur more readily at lower frequency. The width $\Delta\omega$ of the resonance is found to grow with the degree of nonuniformity of particle volumes within a given array, qualitatively

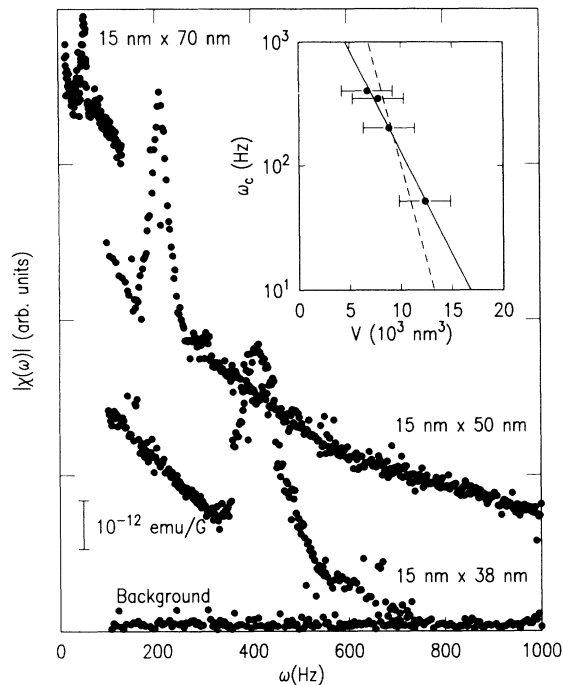


FIG. 1. Frequency-dependent magnetic susceptibility at $T=22.5$ mK of three different arrays of 100 nanometer-scale magnets with interparticle spacings $r=1.0$ μm consisting of structures whose diameters and heights are shown. The curves are arbitrarily displaced vertically with respect to one another. Inset: Theoretical scaling relation between the magnet volume and the observed resonant frequency. The solid line is the best fit, and the dashed line the best fit with $\omega_M \sim 10^{11}$ Hz.

tively consistent with ω_c being a function of volume. This may be seen by comparing in Fig. 1 the data for the array of 15-nm \times 38-nm particles, which were grown manually, with those for the two other arrays, whose growth was computer controlled, and which in consequence have a more uniform particle-size distribution and a correspondingly smaller value of $\Delta\omega/\omega_c$. The inset of Fig. 1 shows $\log_{10}\omega_c$ as a function of the particle volume V for the three arrays of Fig. 1 and one additional array, as a test of the exponential dependence of ω_c on V predicted (as discussed below) to hold for quantum tunneling. The data are reasonably well approximated by a straight line over this limited range of volumes. The temperature dependence of the height of the observed peak for these arrays is shown in Fig. 2. In each case the peak appears at $T \sim 50$ –200 mK, achieving a temperature-independent size at $T \sim 70$ mK, suggestive of the resonance being associated with a quantum-mechanical effect such as magnetic MQT.

It is important to determine whether the resonances are characteristic of the individual magnetic particles, or represent a collective effect of the entire array. Since the interactions between dipoles of moment M_0 vary with their separation r as M_0^2/r^3 , the interaction energy between near-neighbor particles of 15 nm on a side separated by 1.0 μm is equivalent to roughly 30 mK. Thus the interparticle coupling should not start to play a significant role until temperatures comparable to or below the lowest temperature (20 mK) achieved in this experiment. One infers that the observed resonance is likely a property of the individual particles. To test this notion further, we performed susceptibility measurements on an array of similarly sized particles spaced only 0.1 μm apart where the dipolar interactions are 1000 times stronger than in the original array. Here appreciable correlations between the moments on the different magnetic grains should develop at temperatures below roughly $T_0=20$ K. Although the frequency-dependent backgrounds for the 0.1- and 1.0- μm samples were similar, we found no trace of a resonant peak in the 0.1- μm

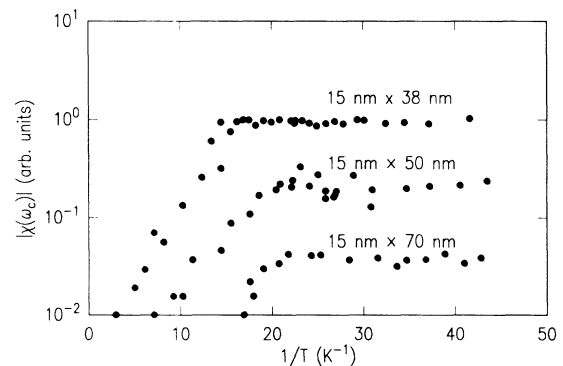


FIG. 2. Temperature-dependent amplitude of the magnetic susceptibility for the structures in Fig. 1.

sample for the entire measured temperature range, $20 \text{ mK} < T < 0.9 \text{ K}$. It is interesting that this suppression of the resonance by interparticle coupling is what one would expect if the origin of the resonance were MQT of the individual magnets. In addition, measurements of the low-frequency ($\sim 11 \text{ Hz}$) susceptibility [Fig. 3(a)] show the magnetization to be essentially constant for $T < 0.9 \text{ K}$, and actually increase with increasing T for $0.7 \text{ K} < T < 0.9 \text{ K}$, suggestive of some kind of magnetic ordering taking place at higher temperature. This is in marked contrast to the $1.0\text{-}\mu\text{m}$ spaced arrays, whose low-frequency susceptibility shows a steady, Curie-like increase (presumably associated with nearly independent, isolated spins or small spin clusters) with decreasing temperature over the entire measured range. This is consistent with the independent particles in these arrays being able to order magnetically only at lower temperature. Furthermore, arrays with $1.3\text{-}\mu\text{m}$ spacing show behavior essentially identical to that of the $1.0\text{-}\mu\text{m}$ arrays.

It is natural to compare these intriguing low-temperature spin dynamics of small magnets with available theoretical results³ for magnetic MQT. In the absence of dissipation,⁸ small magnetic particles in the superparamagnetic regime can be completely described by the operator for the total magnetization, \mathbf{M} , whose magnitude M_0 is proportional to the number of spins N in the particle, i.e., to V . In the presence of magnetic (crystal-

line or shape) anisotropies and/or a magnetic field, the Hamiltonian \mathcal{H} may have minima at two distinct orientations of the vector \mathbf{M} . If \mathbf{M} does not commute with \mathcal{H} , \mathbf{M} will tunnel between the two local-energy-minimum orientations, temporal correlations being given³ by the correlation function

$$S(\tau) \equiv \langle \mathbf{M}(t) \cdot \mathbf{M}(t + \tau) \rangle \sim M_0^2 \cos(2P\tau),$$

where P is the tunneling rate. The imaginary part of $\chi(\omega)$ is proportional to the Fourier transform of $S(\tau)$, $S(\omega)$, through the fluctuation-dissipation theorem, $\chi''(\omega) = (1 - e^{-\hbar\omega/k_B T})S(\omega)/2\hbar$, and thus has a resonance at $\omega = \pm \omega_c \equiv 2P$. The tunneling rate P is conveniently given in the form $P \propto \omega_M e^{-U/k_B T_c}$, where ω_M is a microscopic frequency, U is the energy barrier separating the local minima, and T_c is an effective temperature constructed from M_0 and the anisotropy parameters and applied field. [For the case of an easy x axis and a hard z axis, with respective anisotropy strengths K_x and K_z , e.g., $U = K_x$, and $k_B T_c \sim (K_x K_z)^{1/2}/N$.] Since thermal activation over the barrier proceeds at a rate proportional to the Arrhenius factor $e^{-U/k_B T}$, one expects quantum tunneling to dominate at temperatures $T < T_c$, at which point one anticipates the emergence of the resonant peak at $\omega = \pm \omega_c$ in $\chi(\omega)$. Since the quantity $U/k_B T$ is extensive, the frequency ω_c can be written as $\omega_M e^{-\alpha V}$, where α is independent of volume; hence ω_c decreases exponentially with V . In the presence of an applied magnetic field H , P is predicted² to behave like $P \sim [P_0^2 + (HM_0/\hbar)^2]^{1/2}$, where P_0 is the tunneling rate in zero field.

Within this framework, the ordinate intercept of the line in the inset of Fig. 1 is expected to be ω_M , a microscopic frequency of order 10^{11} Hz . This is very different from the experimental best-fit intercept of $\sim 10^4 \text{ Hz}$. In other words, $\omega_c \ll \omega_M$ implies that ω_c should be extremely sensitive to changes in V ; this sensitivity is not observed experimentally. There are, however, large uncertainties in the effective magnetic volume of the particles, and the best fit to the data with $\omega_M = 10^{11} \text{ Hz}$ (shown as the dashed line in the inset) lies within the error in measurement of the magnet volumes. Moreover, it is likely that the effective magnetic volume is quite different from the measured geometric value, i.e., that not all the spins in a particle contribute to the resonance. Measurements on an array of magnets subsequently covered by an 80-nm gold film revealed little change in the observed resonance, suggesting that the magnetic volume does not extend to the exterior surface. Note that the volumes of the particles within any given array must be identical to $\sim 1\%$ to be consistent with both $\omega_c \sim e^{-\alpha V}$ and the observed narrow widths of the resonances. Such size uniformity is somewhat surprising, though not inconceivable. Within this theoretical picture one can also compute the magnetic anisotropy densities required to produce the measured values of $\omega_c \sim 400 \text{ Hz}$ and $T_c \sim 100 \text{ mK}$ for the $15\text{-nm} \times 50\text{-nm}$ particles. The formula ω_c

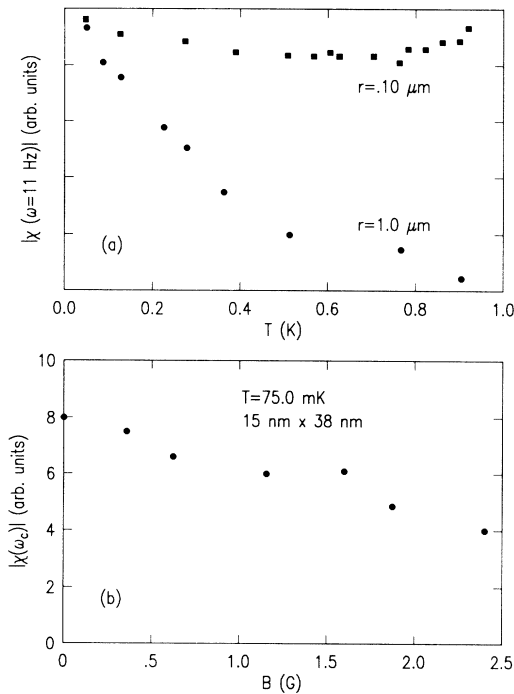


FIG. 3. (a) Low-frequency susceptibility for two arrays of $15\text{-nm} \times 38\text{-nm}$ magnets with different interparticle spacings. The curves are arbitrarily displaced vertically with respect to one another. (b) Integrated magnetic-susceptibility peak as a function of externally applied static magnetic field.

$\sim 2\omega_M \exp[-(K_x/K_z)^{1/2}N]$ yields $K_x \sim 10^2$ ergs/cm³ and $K_z \sim 10^{10}$ ergs/cm³, which are, respectively, 4 orders of magnitude lower and higher than typical bulk crystalline values. While the actual anisotropy energies for such small particles are not known,⁹ even in order of magnitude, they can be extremely large relative to the anisotropies typical of bulk crystalline samples, and change rapidly (even reversing sign) with particle size. The nanometer-scale magnets grown for these measurements are likely to be amorphous rather than crystalline, and their anisotropy is presumably dominated by surface and shape effects.¹⁰ Note too that uncertainties in the volumes affect estimates for the anisotropy strengths in a significant way.

Finally, consider the size and temperature dependence of the resonance in zero field. For temperatures $T \sim 1$ K, and frequencies $\omega \sim \omega_c \sim 400$ Hz, the thermal energy $k_B T$ is large compared with the quantum energy $\hbar\omega_c$: $\hbar\omega_c/k_B T \equiv x \sim 10^{-8}$, so that one is still very much in the classical regime. Thus $\chi''(\omega) \sim (\omega/2T)S(\omega)$, an expression from which \hbar has disappeared, and which remains valid down to roughly $T \sim 10^{-7}$ K. This predicts that the size of the resonance in $\chi(\omega)$ should continue to increase with decreasing T throughout the measured range of temperature, rather than to saturate at about 70 mK. Moreover, $x \ll 1$ implies that the amplitude of the resonance should be immeasurably small. The source of this disparity between theory and experiment is that the observed level splitting $\hbar\omega_c$ is remarkably small compared to all other energies in the problems. This fact is also clearly manifest in the field dependence of the resonance. Theory predicts^{2,11} significant changes in the resonant frequency ω_c for fields of order $\hbar P_0/M_0$, or 10^{-9} G. This extraordinarily small number implies that even stray microgauss fields would produce changes in ω_c of several orders of magnitude, precluding the acquisition of reproducible results even in what is nominally zero field. By contrast, Fig. 3(b) shows the effect of an applied dc field on the amplitude of the resonance. The magnitude decreases steadily with fields up to 2.5 G, extrapolating to zero at ~ 5 G, but no significant shift in ω_c is observed for this range of applied fields. In fact, the milligauss ac fields applied to measure $\chi(\omega)$ are so large relative to $\hbar\omega_c$ that the measurement is not in the linear (small-field) regime. Therefore, even though there

is nominally no external field, these experiments really measure the full nonlinear susceptibility. A satisfactory explanation of the striking experimental observations requires understanding the ramifications of these nonlinearities as well as the role of dissipation in these novel phenomena.

In summary, frequency-dependent magnetic-susceptibility measurements have been made on arrays of nanometer-scale magnets grown with a STM directly within the planar coils of an integrated dc SQUID microsusceptometer. The experimental observations as a function of temperature, particle size, interparticle spacing, and magnetic field reveal new low-temperature spin dynamics in small magnetic systems. While the results are suggestive of magnetic quantum tunneling fundamental discrepancies between the data and theoretical expectations remain.

We would like to thank E. M. Chudnovsky, M. P. A. Fisher, M. R. Freeman, H. R. Krishnamurthy, D.-H. Lee, M. Pomerantz, J. Smyth, and R. A. Webb for helpful discussions, D. Kern and T. Chang for the use of their lithography facilities, and W. J. Gallagher and M. B. Ketchen for fabrication of the SQUID devices.

¹J. Clarke, A. N. Cleland, M. H. Devoret, D. Esteve, and J. M. Martinis, *Science* **239**, 992 (1988), and references therein.

²A. J. Leggett *et al.*, *Rev. Mod. Phys.* **59**, 1 (1987).

³E. M. Chudnovsky and L. Gunther, *Phys. Rev. Lett.* **60**, 661 (1988).

⁴C. P. Bean and J. D. Livingston, *J. Appl. Phys.* **30**, 120S (1959).

⁵D. D. Awschalom *et al.*, *Appl. Phys. Lett.* **53**, 2108 (1988).

⁶M. A. McCord, D. P. Kern, and T. H. P. Chang, *J. Vac. Sci. Technol. B* **6**, 1877 (1988); E. E. Ehrichs, R. M. Silver, and A. L. de Lozanne, *J. Vac. Sci. Technol. A* **6**, 540 (1988).

⁷A. H. Morrish, *The Physical Principles of Magnetism* (Wiley, New York, 1983), p. 370.

⁸Anupam Garg and Gwang-Hee Kim, *Phys. Rev. Lett.* **63**, 2512 (1989).

⁹A. Aharoni, *IEEE Trans. Magn.* **22**, 478 (1986).

¹⁰A. E. Berkowitz, J. A. Lahut, and C. E. Van Buren, *IEEE Trans. Magn.* **16**, 184 (1980).

¹¹L. Gunther (private communication).